

# UNDERSTANDING THE EFFECT OF GLOBAL BUCKLING ON COMPOSITES DAMAGE TOLERANCE

Li, L.<sup>1\*</sup>, Vallée, J.<sup>1</sup>, Shabani, P.<sup>2</sup>, Laliberté, J.<sup>2</sup>, Dondish, A.<sup>3</sup>

<sup>1</sup> Aerospace Research Centre, National Research Council Canada, Ottawa, Canada

<sup>2</sup> Department of Mechanical and Aerospace Engineering, Carleton University, Ottawa, Canada

<sup>3</sup> Department of Mechanical Engineering, Lassonde School of Engineering, North York, Canada

\* Corresponding author (Lucy.li@nrc-cnrc.gc.ca)

**Keywords:** *Global Buckling, Damage Tolerance, Composites Aircraft Materials*

## ABSTRACT

Aircraft structures such as wing are subjected to compressive loading. Buckling, characterized by a sudden out-of-plane deflection of a structural member under compressive loading can lead to structure failure. The goal of this study was to investigate impact resistance and post-damage load carrying capabilities of composite laminates, highlighting the physics of global buckling and its effect on the mechanical strength behaviour. Test standards ASTM D7136 and ASTM D7137 propose a method for low-velocity impact (LVI) and compression after impact (CAI); however, these standards have limitations in the allowable impact energy and subsequent damage size. In this work, larger test panels and new test fixtures were designed and fabricated to study the effects of a wider range of impact scenarios, as well as the buckling behaviour of the composite panels under CAI tests. The experimental results exhibited distinctly different responses of composite panels subject to CAI, where a linear response and higher residual compression strength were observed for the test panels with reduced unsupported area, and a non-linear behaviour and lower compression strength for the larger unsupported area prior to failure. The three-dimensional strain mapping using digital image correlation (DIC) helped build fundamental understanding of the difference in damage mechanisms. This study illustrated the role of global buckling in reducing load-carrying capabilities of composite panels subjected to impact damage at 30J and 75J by as high as 144% and 178%, respectively. This study also illustrated how global buckling is affected by damage onset and propagation mechanisms of composite laminates in compression.

## 1 INTRODUCTION

Fiber reinforced polymer (FRP) laminated materials have been increasingly used in a variety of industry, notably the aerospace, automotive, and wind energy, due to their high specific stiffness and strength, design flexibility, and excellent fatigue resistance. However, their vulnerability to buckling can be a major challenge of their broader applications. Buckling, a phenomenon of unstable deformation of a structural element under compression, has been a subject of many studies [1][2]. The compression after impact (CAI) test is one of the methods for studying compressive strength, damage resistance, and buckling behaviours of composite panels. The test standards ASTM D7136 [3] and ASTM D7137 [4] propose a method for low-velocity impact (LVI) and CAI using 100 mm by 150 mm [4" by 6"] test panels. Studies following these standard dimensions [6][7] have found that the damage propagation initiated at the impact site and the damage growth was driven by shear stresses at the impact dent. Psarras et al. [8] investigated the effects of different panel thickness with multi-site impacts and new support fixtures to suppress global buckling in thin plates. Findings from these studies suggested that the thin plates compression resistance was

## CANCOM2024 – CANADIAN INTERNATIONAL CONFERENCE ON COMPOSITE MATERIALS

more affected by the impacts, while residual strength of the thick panels was less sensitive to impact energy. Limited studies have been carried out to study higher energy levels and larger dents due to limitation of the standard test panel size. Rhead et al. [9] proposed new test fixtures to investigate the different buckling modes on larger panels of 218 mm by 175 mm. This study found that global panel buckling reduced delamination propagation strains and buckling strains and suggested that these reductions indicated a potentially unsafe industry practice of defining allowable strains. Lin et al. investigated the LVI [10] and CAI [11] behavior of laminates with three sizes ranging from 150 mm by 100 mm to 330 mm by 330 mm. In large laminates, global buckling occurred before final failure, resulting in a bilinear force-displacement curve. In addition, in large laminates, delamination mostly occurred near the lateral edges, and the influence of impact damage on the residual compressive strength was found to be less significant.

For this study, modifications were made to ASTM D7136 and ASTM D7137 standards to study the effect of broader range of impact energies while minimizing edge effect. In conjunction with custom-made test fixtures for impact and CAI testing, test panels of 254 mm × 305 mm × 4.3 mm [10" × 12" × 0.171"] were fabricated with IM7/977-3 carbon fiber prepreg and a layup sequence of [0/45/90/-45]<sub>4s</sub>. In addition, anti-buckling support plates were made to reduce the unsupported areas to 127 mm by 178 mm [5" by 7"]. The focus of this paper is on the global buckling and how it affects the failure mechanisms and load-carrying capabilities of the tested composite laminates.

## 2 LOW-VELOCITY IMPACT AND COMPRESSION AFTER IMPACT TESTING

### 2.1 Low Velocity Impact Testing and Post-impact Non-destructive Inspection (NDI)

An INSTRON Dynatup Drop Weight System 8200 was used for impact testing. To accommodate the larger 254 mm by 305 mm [10" by 12"] composite panels, a new test fixture was made with a picture frame of 127 mm by 127 mm [6" by 6"]. Lightly supported boundary conditions were achieved by utilizing four rubber-tip clamps on the bottom plate instead of a top plate. A hemispherical impactor tip of 25.4mm [1"] in diameter and a mass of 6.25 kg was positioned at a calculated height based on the desired impact energy (30 J or 75 J). An ultrasonic C-scan using Tecscan immersion system was performed on the impacted panels at 5 MHz with 12.7 mm [0.5"] flat immersion probe. The C-scan images allows the detection of internal damage such as cavities, delamination, fiber splitting, and other types of damages.

### 2.2 Compression After Impact with Digital Image Correlation

Following the impact, the uniaxial compression test was conducted according to a modified ASTM D7137 test standard [4] using an MTS 661.31A-05 load cell such that the loading direction was orientated in the longitudinal direction parallel to the long edge of 305 mm [12"]. To accommodate the larger panel size, key features from this standard were scaled up and applied to a custom-made CAI fixture. To study the effect of global buckling on the residual compressive strength of the panels, additional front and back anti-buckling supports were machined to reduce the unsupported area to an area of 127 mm by 177.8 mm [5" × 7"]. Figure 1 shows the two test configurations: a) ASTM-equivalent support fixture (NS) that allows for global buckling, and b) Fixture with additional front/back support plates (S) to suppress the global buckling. A combination of four different scenarios for the impact testing and two scenarios for the CAI tests was used for a total of eight different evaluated test conditions as shown in Figure 1c. This test method allows for two options of expected compressive behaviour of test panels, either driven primarily by global buckling or by localized damages.

To evaluate the CAI deformation and strain behaviour of the tested panels, 3D digital image correlation (DIC) was used. To prepare the panels for the DIC, a black base coat of spray paint was applied to the surface before speckling with white paint using an airbrush. Two high-resolution cameras were used for imaging the back side of the sample

CANCOM2024 – CANADIAN INTERNATIONAL CONFERENCE ON COMPOSITE MATERIALS

while another two cameras were imaging the front side [5]. Images from both back and front imaging systems were processed using a commercial DIC software package (DaVis 10.0.3, LaVision GmbH, Göttingen, Germany). The correlation was performed for one frame per second until failure with each frame compared to the first frame of the test to prevent compounding precision errors.

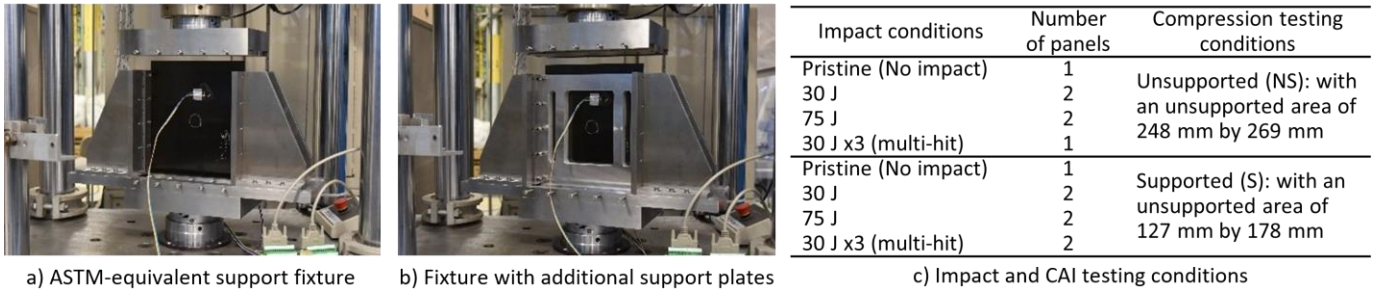


Figure 1. Compression test with a) ASTM-equivalent support fixture (NS) and b) fixture with additional front/back support plates (S). c) Scope of test conditions for impact and compression after impact testing.

### 3 RESULTS

#### 3.1 Drop Tower Impact Testing

Drop tower impact test parameters varied in impact energy resulting in different amounts of post impact damage. With the acquired load data from the drop tower, applied load against time during impact was plotted as shown in Figure 2a. Tests with the same conditions showed great consistency and repeatability. The panels subject to 75J of impact energy had a consistent peak load of around 17 kN and the panels subject to 30J of impact energy had a peak of around 10 kN. The resultant impact damage ranged from no visible damage to significant visible damage. Figure 2b shows the surface level post impact damage difference between the two impact energy levels of 30 J and 75 J, and it also shows the internal damage caused by the impact. Panels hit with 30 J of energy had barely visible damage on the front and back surface, and the panels hit with 75 J had a clear dent at the front with fiber breakage at the back. NDI C-scans from tested panels of 30 J had an average maximum internal damage diameter of 35 mm  $\pm$  2 mm, while panels of 75 J had an average damage diameter of 53 mm  $\pm$  5 mm.

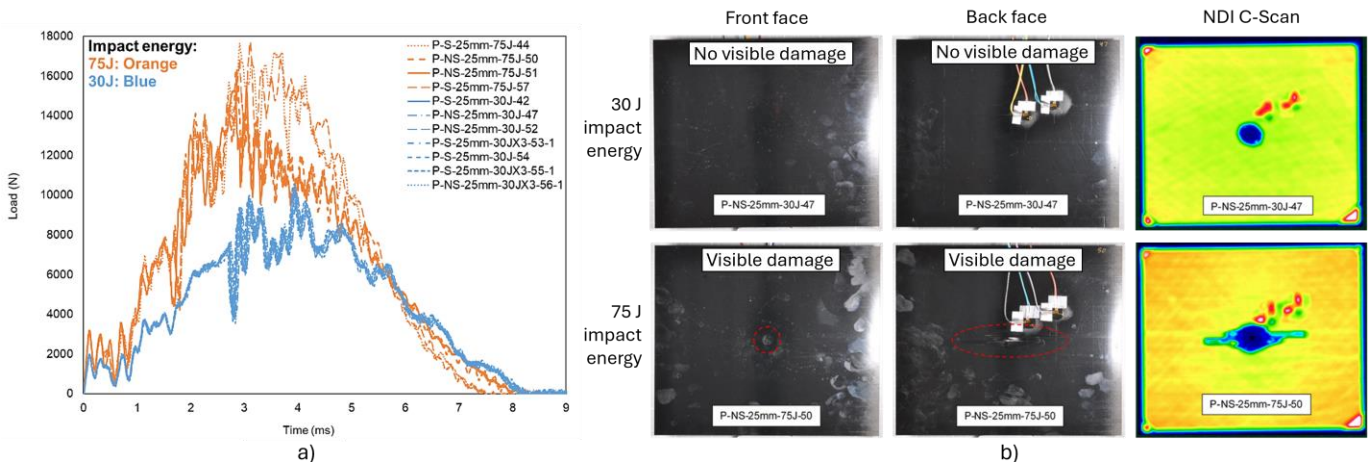


Figure 2. a) Load over time response of panels subject to impact energy of 30J or 75J. b) Post impact images of panels subject to 30J or 75J.

### 3.2 CAI Testing and Post-Compression Damage Analysis

CAI tests were conducted with or without additional anti-buckling plates as shown in Figure 3a. The stress over strain response of the panels subject to CAI were calculated using the applied force and displacement from the load cell and the panel geometry (cross-section area, height of specimen). For the testing without the additional support (NS), a nonlinear response of stress over strain, and a lower ultimate compressive residual strength were observed. In fact, for all non-supported panels, the response became unstable at an average of 90 MPa. Additionally, there is no correlation between the impact damage level and the residual strength of the panels. The pristine specimens and those impacted at 30J or 75J energy levels had an average strength of 193 MPa with no clear distinction in ultimate strength. In comparison, the panels with additional support plates showed a linear response of stress over strain with an increase of ultimate residual strength. There is also a distinction between the results of the different test conditions, where the panels impacted with the higher energy level of 75J reached failure at around 220 MPa, the panels impacted with 30J reached failure at around 250 MPa and the pristine panel had the highest compressive strength and reached failure at around 300 MPa.

Post CAI pictures of the panels are shown in Figure 3b to Figure 3e, which shows the difference in damage propagation between the supported and unsupported panels. Panels that were unsupported had damage propagating from the edges of the panels and off-centered with the impact damage site, whereas the panels that were supported had damage propagating from the impact damage site along the transversal axis of the panel. These results were consistent with all the test scenarios.

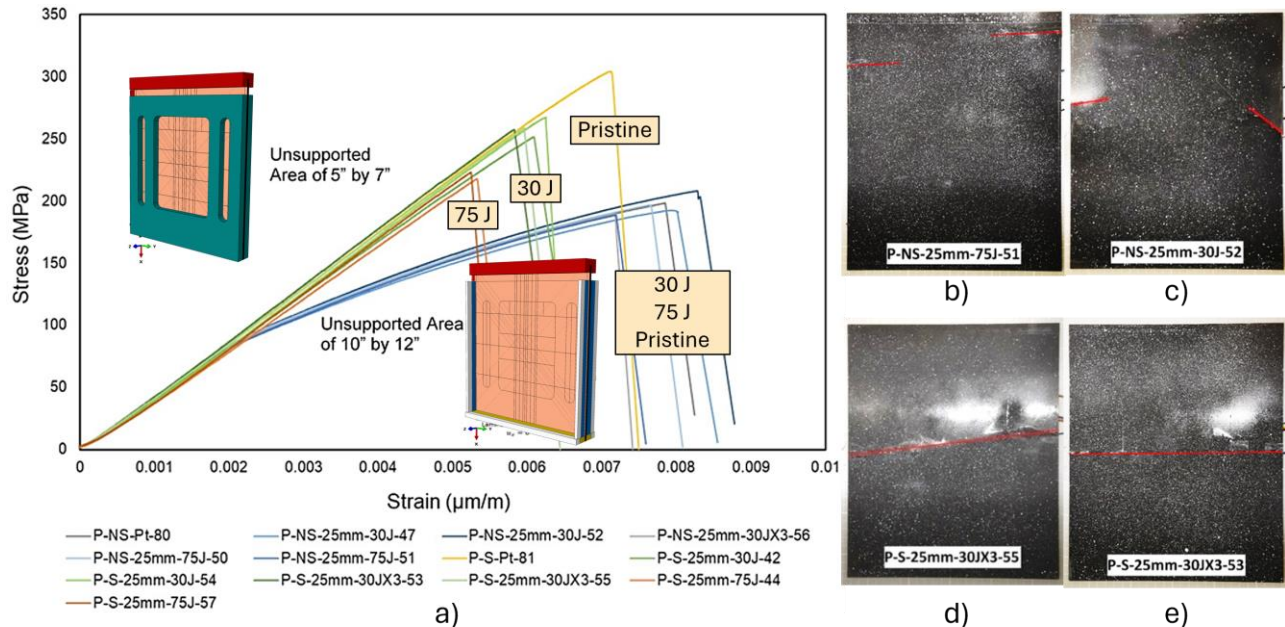


Figure 3. a) Compression after impact response of supported and unsupported panels with different impact energies. Damage propagation mechanisms of b), c) unsupported panels and d), e) supported panels.

### **3.3 Digital Image Correlation of CAI**

From the DIC imaging system, correlation of the speckles was done to evaluate the progression of out-of-plane displacement of the panels when subject to compressive loads. The DIC data of displacement over panel length was plotted to view the progression of the displacement along the y and x axes for both supported and unsupported test conditions. The unsupported panels had a global buckling behaviour where the buckling started just short of the longitudinal edges of the panel. Comparing with the supported scenarios, the support plates constrained the global buckling, and the buckling behaviour was local and limited to 40 mm of the impact site [5].

## **4 DISCUSSION**

### **4.1 Effect of Buckling on Load-Carrying Capabilities of Composites**

Quantifying the difference in compression strength results of the different scenarios can be interpreted in two ways. Looking only at the ultimate stress from Figure 3a, having the additional anti-buckling measure led to an average increase of 11.4% in ultimate compressive residual strength for the 75J, an increase of 29.5% for the 30J, and 55.4% for the pristine panels, when compared with the ASTM-equivalent support fixture. However, if failure is defined as the point where the behaviour of the structure becomes unstable, then the difference in residual strength is even greater. In fact, the panels without the supports became unstable at an average of 90 MPa, compared to the supported panels which stayed stable until the ultimate loads of 220 MPa (after 75J impact) and 250 MPa (after impact at 30J) had been reached, an increase of over 144% and 178%, respectively. This is especially valuable when designing parts that are subject to loads that would make them prone to global buckling. In the aerospace industry, where designs usually rely on the load carrying capabilities of materials, it is important to know the point at which buckling effects lead to a highly nonlinear, unstable material response.

### **4.2 Effect of Global Buckling on Failure Mechanism**

The test results also showed that the buckling mode of the panels had a significant effect on the failure mechanism and damage propagation. In fact, post CAI pictures of the unsupported panels showed that damage growth propagated from the edges of the panels. DIC data confirmed that this effect correlated with the global buckling of these unsupported panels. In comparison, global buckling did not occur with the additional support plates. DIC data and post compression pictures showed that the buckling in these supported panels was local and that the damage propagated from the impact site.

### **4.3 Effects of Impact on Residual Compressive Strength**

The impact damage level had insignificant effect on residual strength in the unsupported panel CAI tests. In fact, no clear distinction can be made between the ultimate compressive strength of pristine panels and the panels impacted with 30J and 75J as shown in Figure 3a. This could be explained by the fact that, under global buckling, the damage propagation originated from the edges of the panel away from the dent site. In contrast, in the supported panels the local buckling correlates to the observable difference in impact energy to compression response. In fact, there is a clear distinction in response between the different impact energies in the supported tests. Pristine panels showed higher compressive residual strength, followed by the panels with an impact energy of 30J and then the panels impacted with an energy of 75J having the lowest residual strength.

## 5 CONCLUSIONS

The goal of this study was to evaluate the effect of global buckling on damage resistance of fiber-reinforced polymers. The test results show the significant effect of the test fixture design on damage behavior and the ultimate compressive residual strength. For some of the tests, global buckling was suppressed through a pair of additional anti-buckling support. This additional anti-buckling measure led to an increase in ultimate compressive residual strength, as compared with the ASTM-equivalent support fixture. For industries where failure is defined as the change in behaviour of mechanical strength of a material, it is valuable to know the point at which the structure becomes unstable. In this study, the panels without the supports became unstable at an average of 90 MPa, compared to the supported panels, which stayed stable until the ultimate load had been reached. This study also shows that the impact damage size had insignificant effect on the CAI strength in specimens that experienced global buckling.

## 6 ACKNOWLEDGEMENT

We would like to thank the technical contributions from Sandra Robertson, Richard Desnoyers, Dmitrii Klishch, Trent Gillis, as well as many others who supported the work. We also would like to acknowledge the financial support of the Department of National Defence Canada for strategic research and development.

## 7 REFERENCES

- [1] X. Wang, J. Huang, R. Tan, Y. Su, Z. Guan, X. Guo, "Experimental investigation on damage mechanisms and buckling behaviors of thin composite laminates in compression after impact", *Composite Structures*, 256: 113122, 2021.
- [2] D. Ghelli, G. Minak. "Low velocity impact and compression after impact tests on thin carbon/epoxy laminates", *Composites Part B: Engineering* 42, no. 7: 2067-2079, 2017.
- [3] D30 Committee, "Test Method for Measuring the Damage Resistance of a Fiber-Reinforced Polymer Matrix Composite to a Drop-Weight Impact Event.", D7136\_D7136M-15.
- [4] D30 Committee, "Test Method for Compressive Residual Strength Properties of Damaged Polymer Matrix Composite Plates.", D7137\_D7137M-17.
- [5] A. Dondish, L. Li and G. W. Melenka, "Full-field deformation and failure analysis for compression after impact of carbon fibre reinforced polymer laminates", *Composite Structures*, Vol. 323, 2023.
- [6] H. Tuo, Z. Lu, X. Ma, J. Xing and C. Zhang, "Damage and failure mechanism of thin composite laminates under low-velocity impact and compression-after-impact loading conditions", *Composites Part B: Engineering*, Vol. 163, pp 642-654, 2019.
- [7] X.C. Sun and S.R. Hallett, "Failure mechanisms and damage evolution of laminated composites under compression after impact (CAI): Experimental and numerical study", *Composites Part A: Applied Science and Manufacturing*, Vol. 104, pp 41-59, 2018.
- [8] S. Psarras, R. Muñoz and M. Ghajari, "Compression performance of composite plates after multi-site impacts: A combined experimental and finite element study", *Composite Structures*, Vol. 322, 2023.
- [9] A.T. Rhead, R. Butler, G.W. Hunt, "Compressive strength of composite laminates with delamination induced interaction of panel and sublaminates buckling modes", *Composite Structures*, Vol. 171, pp 326-334, 2017.
- [10] S. Lin, V. Ranatunga, and A. M. Waas, "Experimental study on the panel size effects of the Low-Velocity Impact (LVI) and Compression After Impact (CAI) of laminated composites, Part I: LVI.", *Composite Structures*, Vol. 296: 115822, 2022.
- [11] S. Lin, V. Ranatunga, and A. M. Waas, "Experimental study on the panel size effects of the low velocity impact (LVI) and compression after impact (CAI) of laminated composites, part II: CAI.", *Composite Structures*, Vol. 295: 115824, 2022.